

Lévy noise induced transitions and enhanced stability in a birhythmic van der Pol system

René Yamapi,^{1,2,*} Raoul Mbakob Yonkeu,³ Giovanni Filatrella,⁴ and Jürgen Kurths^{2,5}

¹*Fundamental Physics Laboratory, Physics of Complex System group,
Department of Physics, Faculty of Science,
University of Douala, Box 24 157 Douala, Cameroon.*

²*Potsdam Institute for Climate Impact Research (PIK), 14473 Potsdam, Germany*

³*Laboratory of Mechanics and Materials,
Department of Physics, Faculty of Science,
University of Yaoundé I, Box 812, Yaoundé, Cameroon.*

⁴*Department of Sciences and Technologies and Salerno unit of CNSIM,
University of Sannio, Via Port'Arsa 11, I-82100 Benevento, Italy.*

⁵*Department of Physics, Humboldt University, 12489 Berlin, Germany.*

(Dated: December 30, 2021)

Abstract

This work describes the effects of Lévy noise on a birhythmic van der Pol like oscillator. Numerical simulations demonstrate that the noise induced escapes from an attractor to another are not markedly different from escapes between stable points in an ordinary potential, albeit the attractors are separated by a barrier of a quasi (or pseudo) potential. However, some differences appear, and are more pronounced when the Lévy distribution index is close to two.

Keywords: Birhythmicity; van der Pol oscillators; Lévy noise; quasi-potential.

PACS numbers:

PACS. 05.40.Fb - Random walks and Levy flights.

PACS. 02.50.Ey - Stochastic processes.

PACS. 02.60.x - Numerical approximation and analysis

PACS. 02.60.Cb - Numerical simulation; solution of equations

PACS. 05.10.Gg - Stochastic analysis methods.

* Author to whom correspondence should be addressed. Electronic mail : ryamapi@yahoo.fr

I. INTRODUCTION

Lévy noise is a preeminent example of non Gaussian noise. The underlying notion is that some noise sources or random signals are not characterized by a finite variance. Moreover, if one makes the further requirement that the noise distribution is stable, that is, it is the limit distribution of the sum of many random and identically distributed variables, the resulting distribution belongs to the family of Lévy functions, as a generalization of the central limit theorem [1]. The presence of anomalous, that is non thermal (Gaussian) noise is widely recognized in physical systems and practical devices. In the natural world, Lévy noise has been modeled for most different systems, from predator-pray [2]. Quite naturally, Lévy noise often appears in telecommunications and networks [3] where noise (from diverse sources as atmospheric disturbances, relay contacts, electromagnetic devices, electronic apparatus, transportation systems, switching transients, and accidental hits in telephone lines [4]) can exhibit impulsive and Lévy-type characteristics. In mechanical systems, Lévy fluctuations have been also used to describe vibration data in industrial bearings [5–7]. Another example of the relevance of anomalous distributions in material issues has been proposed in photoluminescence experiments of moderately doped n-InP samples [8], and the presence of Lévy flights could prove to have an impact on the design of some optoelectronic devices [9]. On the fundamental side Lévy processes can reveal the properties in the electron transport [10] and optical properties [11–13] of semiconducting nanocrystals quantum dots. Transport properties can be connected with Lévy superdiffusion [14], *e.g.* in the quasiballistic heat conduction [15, 16].

A special role is played by Lévy noise in oscillators. Most important for the electrical power grid is the noise from wind turbines rotation parts [17], that can severely affect the infrastructure stability. Also in superconducting active oscillators as superconducting Josephson junctions [18]: Lévy noise has been advocated, for example, in graphene based devices in the form of rare jumps of the voltage response of such non linear oscillator [19] or when the electron-electron interaction of the graphene under the effects of a laser source, gives rise to a random walk with Lévy flights distribution [20]. In nonlinear oscillators the effect of Lévy noise, and indeed of Gaussian noise as well, is subtle, in the sense that the stable solution is a dynamical attractor. When this is the case, and the force cannot be derived as the gradient of a potential function, the problem of the stability cannot be deduced from the standard escape from a potential well, characterized by an *Arrhenius* behavior of the lifetime (as a function of the noise intensity). However, an alternative approach based on the concept an effective potential (a pseudo, or quasi-potential) has proved effective to

treat the consequences of noise on the metastable periodic attractor for nonlinear oscillators as Josephson junctions [21–23] and for van der Pol birhythmic oscillators [24–26], also in the presence of correlated noise [27]. It is therefore quite natural to imagine to extend the theory of Lévy noise induced escapes from ordinary potentials [28, 29] to quasi-potentials for birhythmic van der Pol like systems. In doing so, one follows in the essence the approach (for monorhythmic systems) already employed using the principle of minimum action [30, 31], that describes a numerical method to derive the quasi-potential for a non gradient system. The conceptual difficulty to follow this line of reasoning is that the distance rather than the energy barrier matters. Moreover, this line of research is numerically heavy. An analytic approach has been presented for the ordinary, non birhythmic, van der Pol system (with Lévy noise) [32], and also extended to a birhythmic system [33].

In this work we use the numerical method already employed for Gaussian noise, that is to revert the logic of the escape time in the presence of Lévy noise [57, 58]. In doing so one wishes to determine if the quasi-potential concept is applicable to birhythmic system, and the limits of the applicability of such concept. Also, one wishes to ascertain if numerical simulations can carry information about the theoretical estimates of the features of escapes from ordinary potentials, for instance the dependence of the escape times on the Lévy index, α .

The paper is organized as follows. Sect. II describes the birhythmic van der Pol system driven by Lévy noise and the algorithm of the numerical simulations. After the description of the main features of the deterministic birhythmic van der Pol oscillator and the parameter region where birhythmicity appears. The Lévy's process and numerical algorithm conclude this section. In Sect. III, we focus on numerical computed escape rates and the algorithm to generate random Lévy noise and to integrate the stochastic differential equation. For low noise regime, the Arrhenius factor (*i.e.*, the relation between the escape time T_{esc} and the noise intensity D) allows to determine an effective activation energy barrier ΔU from the slope of the linear part of the variation in the escape time versus the inverse noise intensity. Section IV is devoted to conclusions.

II. THE STOCHASTIC BIRHYTHMIC SYSTEM AND LEVY'S PROCESS

A. The birhythmic van der Pol system

The model considered is a van der Pol-like oscillator with a nonlinear function of higher polynomial order described by the following nonlinear equation (overdots as usual stand for the derivative with respect to time)

$$\ddot{x} - \mu (1 - x^2 + \alpha x^4 - \beta x^6) \dot{x} + x = 0, \quad (1)$$

where the quantities α and β are positive parameters indicate the system behavior to a ferroelectric instability compared with its electrical resistance, while μ is a positive parameter that tunes nonlinearity [34–37]. Eq. (1) describes several dynamic systems, ranging from physics to engineering and biochemistry [37–39]. In particular Eq. (1) seems to be more appropriate for some biological processes than the classical van der Pol oscillator, as shown by Kaiser in Ref. [40]. When employed to model biochemical systems, namely the enzymatic-substrate reactions, x in Eq. (1) is proportional to the population of enzyme molecules in the excited polar state. Model (1) is therefore a prototype for self-sustained systems and exhibits some interesting features of nonlinear dynamical systems; for instance Ref. [34, 35] have analyzed the super-harmonic resonance structure and have found symmetry-breaking crisis and intermittency. The nonlinear dynamics and the synchronization process of two such systems have been recently investigated in Ref. [36, 37], while the possibility that introducing an active control of chaos can be tamed for an appropriate choice of the coupling parameters has been considered in Ref. [38]. Recently, we have found in ref. [27] the effects of external excitation on the multi-limit cycle van der Pol system. It appears that the birhythmic behavior is still present for a very small excitation and disappear when the amplitude of the driven becomes large.

The nonlinear self-sustained oscillator Eq. (1) possesses more than one stable limit-cycle solution [40], a condition for the occurrence of birhythmicity. Birhythmic systems are of interest, for example in biology, to describe the coexistence of two stable oscillatory states, a situation that can be found in some enzyme reactions [41]. Another example is the explanation of the existence of multiple frequency and intensity windows in the reaction of biological systems when they are irradiated with very weak electromagnetic fields [35, 40, 42–45]. In this work we will focus on model (1) as a prototype for the occurrence of birhythmicity.

$AS_i = (a, \beta)$	Amplitudes	Quasi-potential barriers ΔU_i
$AS_1 = (0.114, 0.003)$	$A_1 = 2.37720$ $A_2 = 5.02638$ $A_3 = 5.46665$	$\Delta U_1 = 1.062 \times 10^{-2}$ $\Delta U_3 = 2.111 \times 10^{-4}$
$AS_2 = (0.1, 0.002)$	$A_1 = 2.3069$ $A_2 = 4.8472$ $A_3 = 7.1541$	$\Delta U_1 = 1.437 \times 10^{-2}$ $\Delta U_3 = 4.423 \times 10^{-2}$
$AS_3 = (0.12, 0.003)$	$A_1 = 2.4269$ $A_2 = 4.2556$ $A_3 = 6.3245$	$\Delta U_1 = 4.989 \times 10^{-2}$ $\Delta U_3 = 2.372 \times 10^{-2}$
$AS_4 = (0.13, 0.004)$	$A_1 = 2.4903$ $A_2 = 4.4721$ $A_3 = 5.0791$	$\Delta U_1 = 4.342 \times 10^{-3}$ $\Delta U_3 = 4.237 \times 10^{-4}$

Table I: Amplitudes of the limit cycles and quasi-potential barriers $\Delta U_{1,3}$ for the asymmetric potential. All data refer to the case $\mu = 0.01$ and $D = 0.0$. All the results are obtained analytically.

$S_i = (a, \beta)$	Amplitudes	Quasi-potential barriers ΔU_i
$S_1 = (0.0675, 0.0009)$	$A_1 = 2.1730001$ $A_2 = 6.3245003$ $A_3 = 8.6760004$	$\Delta U_1 = 6.5085 \times 10^{-2}$ $\Delta U_3 = 6.5085 \times 10^{-2}$
$S_2 = (0.1635, 0.007)$	$A_1 = 3.0925001$ $A_2 = 3.5280002$ $A_3 = 3.9190002$	$\Delta U_1 = 2.376 \times 10^{-5}$ $\Delta U_3 = 2.445 \times 10^{-5}$
$S_3 = (0.16, 0.00658)$	$A_1 = 2.9520001$ $A_2 = 3.5965002$ $A_3 = 4.1535002$	$\Delta U_1 = 1.0345 \times 10^{-4}$ $\Delta U_3 = 1.1011 \times 10^{-4}$
$S_4 = (0.1476, 0.0053)$	$A_1 = 2.6905001$ $A_2 = 3.8525002$ $A_3 = 4.7405002$	$\Delta U_1 = 8.6713 \times 10^{-4}$ $\Delta U_3 = 8.7677 \times 10^{-4}$

Table II: Amplitudes of the limit cycles and quasi-potential barriers $\Delta U_{1,3}$ for the symmetric potential. All data refer to the case $\mu = 0.01$ and $D = 0.0$. All the results are obtained analytically.

Following Refs.[36, 37], the periodic solutions of Eq. (1) can be approximated by

$$x(t) = A \cos \omega t. \quad (2)$$

The analytic amplitude A and frequency ω can be readily obtained [36, 37]. It has been found that the amplitude A is independent of the parameter μ , which only enters in the frequency w . The amplitude equation is given by

$$\frac{5\beta}{64}A^6 - \frac{\alpha}{8}A^4 + \frac{1}{4}A^2 - 1 = 0, \quad (3)$$

and ω is given by:

$$\omega = 1 + \mu^2 \omega_2 + o(\mu^3), \quad (4)$$

with

$$\omega_2 = \frac{93\beta^2}{65536}A^{12} - \frac{69\alpha\beta}{16384}A^{10} + \left(\frac{67\beta}{8192} + \frac{3\alpha^2}{1024}\right)A^8 - \left(\frac{73\beta}{2048} + \frac{\alpha}{96}\right)A^6 + \left(\frac{1}{128} + \frac{\alpha}{24}\right)A^4 - \frac{3}{64}A^2.$$

Depending on the value of the parameters α and β , the van der Pol birhythmic system possesses one or three limit cycles. We find that depending on the values of the parameters α and β , the modified van der Pol equation (1) possesses one or three limit cycles. When three limit cycles are obtained, two of them are stable and one is unstable, a condition for birhythmicity; the unstable limit cycle represents the separatrix between the basins of attraction of the two stable limit cycles. This appear in Fig. 1 where the bifurcation lines that contour the region of existence of birhythmicity in the two parameter phase space $(\alpha - \beta)$ [36, 37]. The bifurcation line on the left denotes the passage from a single limit cycle to three limit cycles, while the right line denotes the reverse passage from three limit cycles to a single solution. At the conjunction, a codimension-two bifurcation, or cusp, appears. The first bifurcation encountered increasing the amplitude A corresponds to the saddle-node bifurcation of the outer or larger limit cycle amplitude, while the second bifurcation occurs in correspondence of a saddle-node bifurcation of the inner or smaller amplitude cycle. The two frequencies associated with the limit cycles are very similar close to the lowest amplitude A bifurcation and clearly distinct at the highest α bifurcation line. In Figure 1 is shown the range of existence of birhythmic solutions in the parameter plane (α, β) ; examples of the corresponding pseudo-potential is shown in Figure 3: i) the first type is an asymmetric pseudo-potential with different potential wells (such as in Fig.3(i)); ii) and the second type is a symmetrical potential (see Fig.3(ii)) and here the depths of the two potential wells are almost identical. In Tables I and II are reported the amplitudes of the limit cycles in both cases, for some selected values of α and β . The two sets of parameters: AS_1 for the asymmetric quasi-potential and S_1 for the symmetric quasi-potential are considered in this work.

B. The Lévy process representation

Lévy distributions, that describe the noise we consider in this work, are a rich class of probability distributions with several intriguing mathematical properties [46]. The Lévy process can be

viewed as a generalized Wiener process that follow the Lévy distribution $L_{a,b}(\zeta, \sigma, \delta)$; the representation is given by the characteristic function defined in the Fourier transform $\Phi(k)$ [47]:

$$\Phi(k) = \begin{cases} \exp \{ i\delta k - \sigma^a |k|^a (1 - ib \operatorname{sgn}(k) \tan(\frac{a\pi}{2})) \} & \text{for } a \neq 1, 2, \\ \exp \{ i\delta k - \sigma |k| (1 + ib \frac{2}{\pi} \operatorname{sgn}(k) \ln |k|) \} & \text{for } a = 1, \\ \exp \{ i\delta k - \frac{1}{2} \sigma^2 k^2 \} & \text{for } a = 2, \end{cases} \quad (5)$$

where a ($0 < a \leq 2$) denotes the stability Lévy index; for $a = 2$ the Lévy stable distribution is the standard Gaussian distribution. The parameter b ($b \in [-1; +1]$) is an asymmetry, or skewness parameter, namely, the Lévy distribution is symmetric for $b = 0.0$ and asymmetric for $b \neq 0.0$, δ ($\delta \in \mathbb{R}$) is the center or location parameter which denotes the mean value of the distribution, and the mean of the distribution exists and reads δ as $1 < a \leq 2$ [47]. The parameters σ ($\sigma \in]0; +\infty[$) and $D = \sigma^a$ are the scale parameter and noise intensity, respectively [48]. The intensity of the Lévy noise is determined by the parameter D ; if the van der Pol oscillator is used to describe the ferroelectric oscillations, D has the physical meaning of the measure of the intensity of the random electric field.

The random variables ξ corresponding to the characteristic functions (5) can be generated by the algorithm presented in Refs. [49, 50] as follows: first one generates the random variables U uniformly distributed on $[-\frac{\pi}{2}, +\frac{\pi}{2}]$ and the variable W exponentially distributed with a unit mean; U and W being statistically independent. The Lévy distributed variable X can be generated as follows:

For $a \neq 1$:

$$X = S_{a,b} \frac{\sin(a(U + B_{a,b}))}{(\cos(U))^{1/a}} \left(\frac{\cos(U - a(U + B_{a,b}))}{W} \right)^{\frac{1-a}{a}}, \quad (6)$$

where

$$\begin{cases} B_{a,b} = \frac{\arctan(b \tan(a\pi/2))}{a}, \\ S_{a,b} = (1 + (b \tan(a\pi/2))^2)^{\frac{1}{2a}}. \end{cases} \quad (7)$$

For $a = 1$:

$$X = \frac{2}{\pi} \left[\left(\frac{\pi}{2} + bU \right) \tan U - b \log \left(\frac{a\pi W \cos U}{2bU + a\pi} \right) \right]. \quad (8)$$

Finally, the abovementioned ξ reads:

$$\xi = \begin{cases} \sigma X + \delta, & a \neq 1, \\ \sigma X + 2b\sigma \frac{\log(\sigma)}{2} + \delta, & a = 1. \end{cases} \quad (9)$$

The Lévy noise is a formal time derivative of the generalized Wiener process. For the time step of integration Δt , the increments of the generalized Wiener process are distributed according to the distribution $L(\xi, \sigma \Delta t^{1/a}, \delta)$. The Lévy process can be retrieved with the transformation $\zeta(t) = \Delta t^{1/a} \xi$ [49, 50]. Lévy probability densities functions under different stability indexes and skewness parameters are presented in Fig.2, symmetric for $b = 0$; for $a < 1$, $L(\zeta, \sigma \Delta t^{1/a}, \delta)$, left-skewed for $b < 0$ and right-skewed for $b > 0$. For $a > 1$, $L(\zeta, \sigma \Delta t^{1/a}, \delta)$ is right-skewed for $b < 0$ and left-skewed for $b > 0$.

C. The numerical method to simulate the birhythmic van der Pol system driven by Levy noise

Let us consider the multi-limit-cycle van der Pol-like oscillator to model coherent oscillations in biological systems, such as an enzymatic substrate reaction with ferroelectric behavior in brain waves models (see Ref.[37, 51, 52] for more details). In this case, one should include the electrical field applied to the excited enzymes, which depends for example on the external chemical influences (*i.e.*, the flow of enzyme molecules through the transport phenomena). One can therefore assume that the external chemical influence and the dielectric contain a random perturbation. Therefore, adding both the chemical and the dielectric contribution, the activated enzymes are subject to a random excitation governed by the Langevin version of Eq. (1), namely:

$$\ddot{x} - \mu(1 - x^2 + \alpha x^4 - \beta x^6)\dot{x} + x = \zeta(t), \quad (10)$$

where $\zeta(t)$ denote Lévy noise and is the formal time derivative of a Lévy process $\xi(t)$, which can be viewed as a generalized Wiener process, obeying to the Lévy distribution $L(\xi, \sigma \Delta t^{1/a}, \delta)$. We recall that the Lévy noise measure the intensity of the random electrical field. By introducing the new variable $\dot{x} = u$, equation (10) can be write in the form:

$$\begin{cases} \dot{x} = u, \\ \dot{u} = \mu(1 - x^2 + \alpha x^4 - \beta x^6)u - x + \zeta(t), \end{cases} \quad (11)$$

and the relative difference scheme [46] is obtained to calculate: system (11):

$$\begin{cases} x_{n+1} - x_n = u_n \Delta t, \\ u_{n+1} - u_n = [\mu(1 - x_n^2 + \alpha x_n^4 - \beta x_n^6)u_n - x_n] \Delta t + \Delta t^{1/a} \xi, \end{cases}$$

where ξ denotes Lévy distributed random number with the stability Lévy index a and the noise intensity $D = \sigma^a$. For the sake of simplicity and uniform, all our simulations are performed with

the time step $\Delta t = 0.01$. In this work we only consider the case $\delta = b = 0$, *i.e.* the symmetric Lévy distribution.

III. GLOBAL STABILITY ANALYSIS

A principal question about the effects of noise is the occurrence of large deviations, that is excursions from an attractor to another. In fact, an attractor is only locally stable, but for birhythmicity to be actually displayed one might be interested in the global analysis, that is the time spent on average in the proximity of each attractor. The approach for potential systems, that is when the force can be derived from the gradient of a function, one can refer to the classical Kramers theory, with the many modifications that have been developed. For non-gradient systems, the quasi-potential plays a similar role, for it determines the asymptotic low noise limit for Gaussian noise [53]. The quasi-potential has proved effective for van der Pol birhythmic system driven by uncorrelated and correlated Gaussian noise, also in the presence of a sinusoidal forcing term [24, 26, 54, 55]. Our goal is to determine whereas the same approach can be effective for Lévy noise.

A. Statement of the problem

A quasi-potential function $U(A)$ is an effective energy in the sense that it determines in the low noise regime, the escapes from the attractor with an Arrhenius-like behavior [25]:

$$\langle T \rangle \propto \exp(\Delta U/D). \quad (12)$$

A number of questions arise in the extension of Eq.(12) to birhythmic van der Pol under Lévy noise influence. First, one can ask how to modify the functional form of Eq.(12). The escapes are governed, for Lévy noise systems with a bona fide potential [56–58]:

$$\langle T_{esc}(a, D) \rangle = \left(\frac{\eta^{1-\mu_a} \Delta x^{2-2\mu_a+a\mu_a}}{4^{1-\mu_a} \Delta U^{1-\mu_a} 2^{a\mu_a}} \right) \frac{\mathcal{C}_a}{D^{\mu_a}}, \quad (13)$$

where Δx is the distance between the stable minimum of the potential and the separatrix, ΔU is the energy or activation barrier, η is the damping index (that only appears to correctly normalize the overdamped equation), a the index of the Lévy distribution, D the noise intensity. The scaling exponent μ_a and the coefficient \mathcal{C}_a are supposed to have a universal behavior for overdamped

systems [57], such as:

$$\mu_a \simeq 1 + 0.401(a - 1) + 0.105(a - 1)^2. \quad (14)$$

The adaptation of Eq.(13) to the van der Pol birhythmic system gives a first analytical result on the influence of Lévy noise. In other words, in Eq.(13) x is a generic coordinate where the force stems from a potential. As such, x cannot be the variable of Eq.(5), that is a non-potential (or non-gradient) ordinary differential equation, and hence U does not exist. To apply the theory of Lévy noise [28, 29] to Eq.(5) it is necessary to introduce a quasi-potential that plays the role of U . Also, the dynamic variable can presumably change, and is not any more x .

The form of the quasi-potential has been derived with the stochastic averaging method for Gaussian noise. How to calculate the same potential for Lévy noise is still an open problem. As a first guess, let us assume that it is the same potential as in the case of the Gaussian noise:

$$\frac{dA}{dt} = -\frac{dU(A)}{dA} + \sqrt{\tilde{D}}\zeta_1(t), \quad (15)$$

where A is a generic coordinate, e.g. the amplitude A of the oscillations as per Eq.(2), $\zeta_1(t)$ is the Gaussian noise, \tilde{D} an effective noise amplitude ($\tilde{D} = D/\omega^2$ in Ref. [26]) and the effective potential $U(A)$ is given by [26]:

$$U(A) = \frac{\mu}{128} \left(\frac{5\beta}{8}A^8 - \frac{4\alpha}{3}A^6 + 4A^4 - 32A^2 \right) - \frac{\tilde{D}}{2} \ln(A). \quad (16)$$

As mentioned, a first rough approach could be to assume $D = 0$ in Eq.(16). This choice corresponds to take the deterministic averaging. The first possibility is therefore the following: to use Eq.(13), where the amplitude A replaces x , and consider $U(A)$ as the quasi-potential. In this approximation, Δx , the distance with the separatrix, becomes $A_2 - A_1$ and $A_3 - A_2$ for the outer and inner barriers, respectively. In this approximation, the damping reads $\eta = 1$. Shortly, one could apply the theory of Checkin to Eq.(15) with $\zeta_1(t)$ a Lévy noise. This is a very rough approximation, but gives an analytical prediction to be compared with numerical data.

There are other possibilities. One is to use the principle of minimum action [30, 31]. These authors describe a numerical method to derive the quasi-potential for a non gradient system. The physical idea, that has also been used for Josephson junctions [22, 23], is that noise activated trajectories have a different weight, and that the minimum energy is the most likely to be followed by the noise driven system. However, this line of research is numerically heavy, and might also prove not appropriated for Lévy noise, where the distance rather than the energy barrier matters.

A more promising avenue is perhaps to repeat the calculations for the ordinary van der Pol system (with Lévy noise) of Ref. [32]. In particular in the paper "The exit problem from the neighborhood of a global attractor for heavy-tailed Lévy diffusions", in Sect. 2.4 it is presented the application of the method. Interestingly, in a paper on a similar subject, "Metastability of Morse-Smale dynamical systems perturbed by heavy-tailed Lévy type noise", the same authors also consider the birhythmic system of Moran and Goldbeter [33], Sect. 2.4. The calculations on this birhythmic system with two attractors is specifically considered to derive a quasi-potential rather than an ordinary potential.

Finally, one could use the numerical method already employed for Gaussian noise, that is to revert the logic of Eq. (13) to determine the energy activation. This approach leads to the following definition of quasi-potential:

$$\Delta U \equiv \frac{\eta}{4} \left(\frac{\Delta x^{2-2\mu_a+a\mu_a}}{\langle T_{esc}(a, D) \rangle 2^{a\mu_a}} \right)^{\frac{1}{1-\mu_a}} \left(\frac{\mathcal{C}_a}{D^{\mu_a}} \right)^{\frac{1}{1-\mu_a}}. \quad (17)$$

This procedure is rather cumbersome, for Lévy escapes are almost independent of the potential height, that only appears in the prefactor of Eq.(13). It is anyway interesting to verify if, and to which extent, the behavior of Eq. (13) is reproduced by the numerically retrieved confining energy. The prefactor is the most delicate point in the calculations [32]. To underline the effects, one can rewrite Eq. (13) as follows :

$$\log [\langle T_{esc}(a, D) \rangle] = \log \left[\frac{\eta^{1-\mu_a}}{4^{1-\mu_a} 2^{a\mu_a}} \right] + \log \left[\frac{\Delta A^{2-2\mu_a+a\mu_a}}{\Delta U^{1-\mu_a}} \right] + \log [\mathcal{C}_a] - \mu_a \log [D]. \quad (18)$$

As $\mu_a \simeq 1$ when the barrier is changed the main contribution arises from ΔA . This also could be checked numerically, using Tables I,II for the distance ΔA , possibly completed with the barrier heights ΔU .

However, the very fact that the escapes follow the functional form of a power law (rather than an exponential), as shown in the numerical calculations is *per se* of interest.

B. Escape times from the periodic attractors

To examine the escape times from the periodic attractors caused by the Lévy noise term in Eq.(9) that induces the system to occasionally jump from one limit cycle to the other. The system, initially on a limit-cycle attractor with amplitude A_1 or A_3 , is forced by the random fluctuations to leave the attractor and to wander about in the neighboring state space. Escape occurs when this

<i>Levy index a</i>	$T_{esc}(A_1 \rightarrow A_3)$		$T_{esc}(A_3 \rightarrow A_1)$	
0.1	755.96	12.58	1465.57	36.435
0.25	972.61		1669.03	
0.5	1510.22		2018.27	
0.75	2540.22		1199.91	
1.0	4064.31	296.5	1603.60	1783.9
1.25	5884.04		1261.42	
1.5	10938.01		1032.77	
1.75	24587.66		780.55	
1.9	73130.41		589.92	
1.99	1024791.23	1118979.9	482.99	39468200.705
2.0	14650719.12		492.74	

Table III: *Escape times for the asymmetric pseudo-potential with low noise intensity $D = 0.001$. All data refer to the case $\mu = 0.01$.*

GF: I assume these are the numerical escape times. Could you also insert the analytical estimates?

random motion drives the system across the boundary of the basin of attraction or the unstable limit cycle with amplitude A_2 , (*i.e.* $|x| > A_2$ (respectively, $|x| < A_2$)) over the activation energy ΔU_1 (respectively, ΔU_3). This energy is provided by the random force, that thus furnishes the energy equivalent to the depth of the left (respectively, right) well of the bistable potential. The mean escape times T_{esc} for the transitions $A_1 \rightarrow A_3$ and $A_3 \rightarrow A_1$ as function of the noise intensity D for the asymmetric and symmetric pseudo-potentials are shown in Figs. 6 and 7 for several different values of the Lévy index a ($0.1 \leq a \leq 2$). We generally observe that for both types of potential, the curves for $\alpha < 2$ obey a different law in comparison to their Gaussian counterpart. Earlier studies have shown that the variation of the escape time will depend on the regime of the noise intensity to be considered. For low noise intensity regime, in addition to the exponential dependence of the inverse of the intensity of the noise, $1/D$, as it appears on Figs.4,5. We present in Figs. 6,7 a power-law asymptotic behavior, as predicted by Eq. (13). The figures refer to both the symmetric and asymmetric cases of the pseudo-potentials. A thorough analysis of the data of the results presented in Figs. 6 and 7 allows us to show the dependencies of the coefficient C_a and the power-law exponent μ_a on the Lévy index a in Figs.8 and 9, respectively. In Fig. 8

<i>Levy index</i> a	$T_{esc}(A_1 \rightarrow A_3)$		$T_{esc}(A_3 \rightarrow A_1)$	
0.1	772.78	16.70	1635.57	23.39
0.25	1002.05		2321.54	
0.5	1737.14		7259.01	
0.75	2980.91		10192.21	
1.0	5377.62	189.18	13095.21	333.99
1.25	9136.22		13629.12	
1.5	20332.91		49020.82	
1.75	64860.04		43477.14	
1.9	36221.74		404335.44	
1.99	2326787.54	18133.63	2957929.24	560387.519
2.0	1422.24		233281.25	

Table IV: *Escape times for the symmetric pseudo-potential with low noise intensity $D = 0.001$. All data refer to the case $\mu = 0.01$.*

GF: I assume these are the numerical escape times. Could you also insert the analytical estimates?

the coefficient C_a theoretical behavior reads [29] 1 for $a \rightarrow 0$, passes through $\pi/2$ for $a = 1$, and diverges as $1/(2-a)$ as the Lévy parameter approaches 2. This qualitative behavior is very roughly reproduced by the data of Fig. 8, that does not start from 0 as expected for $a \rightarrow 0$, reads 1 instead of $4\pi/5$ for $a = 1$, and diverges more mildly than expected. Note that for our numerical investigation, C_a reads 0.15 for the index parameter approaches 0.01. In Fig.9, the dependence of the scaling exponent μ_a versus the Lévy index, a are compared to the analytical approximation (14). For both symmetric and asymmetric pseudo-potential, the estimate is acceptable. One can conclude that the prefactor C_a is only qualitatively captured by the estimate for the ordinary potential, while the scaling exponent μ_a seems to be closer to the ordinary potential predictions.

The influence of the noise intensity on the escape process is shown in Figs. 10,11 as the dependence of the mean escape time T_{esc} versus the Lévy index a , for several different values of the noise intensity, D , for the asymmetric and symmetric pseudo-potential.

GF: could you add in the figures the predictions of Eq.(18)?

As it is often the case, increasing the noise intensity reduces the escape time in both types of potential. However, these observations strongly depend on the Lévy index a ; it appears hat for a

very small value of the intensity of the noise, for example $D = 0.001$, the escape time increases or decreases considerably when the Lévy index is close to 2, that is close to the Gaussian case. For example, in the case of the asymmetric pseudo-potential, the escape transition time $T_{esc}(A_1 \rightarrow A_3)$ (or $T_{esc}(A_3 \rightarrow A_1)$) when the Lévy index changes from 0.1 to 2, the escape time passes from 755 to 14650719 (from 1465 to 492.4, respectively). This is reported in Table III, that displays the dependence of the escape times as a function of the Lévy index. In the case of symmetric pseudo-potential, one observes the same behavior when the Lévy index increases, see Table IV for a much more in-depth look at the dependence of escape time versus the Lévy index, a . It should be noted that in this case the pseudo-potential is initially symmetric without the Lévy noise term, (*i.e.* $T_{esc}(A_1 \rightarrow A_3) \equiv T_{esc}(A_3 \rightarrow A_1)$), becomes asymmetric with the presence of this noise. It can be seen that when the Lévy index a increases from 0.1 to 2.0, the escape time to leave the pseudo-potential well around the limit cycle amplitude A_3 increases very considerably and makes the attractor A_3 more stable under the effect of the Lévy noise. As a result, a particle confined in this pseudo-potential remains for a very long time under the effects of the random fluctuations induced by the Lévy noise.

Numerical simulations can be used to show the effect of the Levy index a on the pseudo-potential associated with Eq. (13), that is on the global stability properties of the attractors. In other words, one can estimate from numerical simulations the average time that a particle confined in the potential well spends to move to the other well. The analytic approximations developed in the previous subsection can thus be checked against the numerical results. A discrepancy is to be expected, for the theory of the Lévy noise has not been fully extended to the pseudo-potentials. Fig. 12 presents the comparison between the numerical studies and the analytical results, for the transitions in the two cases of symmetric and asymmetric pseudo-potentials. It appears in the data that the comparison between the analytical and numerical results is acceptable for the Lévy $a = 0.1$, but the agreement progressively deteriorates when the index a increases.

C. Estimate of the effective energy barriers and residence times of the attractors

To determine the effective energy barriers, $\Delta U_{1,3}$, it is important to notice from the behavior of the type reported in Fig. 6 that there exist different regimes for the dependence of the escape times T_{esc} , depending on the Lévy noise parameters. For example, in the low noise intensity regime, the data in Fig. 4 and 5 exhibit an exponential behavior of the escape time T_{esc} as a function of the

<i>Levy index a</i>	$\frac{\Delta U_1}{\Delta U_3}(AS_1)$	$\frac{\Delta U_1}{\Delta U_3}(S_1)$
0.1	1.2	1.22
0.25	2.22	1.57
0.5	1.006	0.94
0.75	1.29	1.24
1.0	1.2	0.921
1.25	1.27	0.85
1.5	1.2	0.84
1.75	1.58	1.58
1.85	1.512	1.068
1.9	2.34	0.87
1.95	3.9	0.67
1.99	7.26	0.617
2.0	3.23	0.58

Table V: Dependencies of the ratio $\Delta U_1/\Delta U_3$ versus the Lévy index a for the asymmetric (AS_1) and symmetric (S_1) pseudo-potentials.

inverse noise intensity, $1/D$.

GF: I am not sure that the figures as they are now are sufficient to demonstrate the behavior that is here described. Also, it is not clear the procedure, I have tried to add some details, please complete the description. Moreover, for Lévy flights equation (12) does not hold, one should use (13). Finally, it might be interesting to check other quantities that are not ΔU .

Fitting a straight line through the data points in the linear part of Eq. (12) and measuring its slope, we obtain an estimate of ΔU_1 and ΔU_3 , the effective activation energies for the escape from the limit-cycle attractors A_1 and A_3 , respectively. We have determined and shown in Figure 13 the dependencies of the energy barriers on the Lévy index a , for the escape transitions $A_1 \rightarrow A_3$ and vice versa. We note that when we add the Lévy noise term on Eq. (10), the symmetric properties of the pseudo-potentials are less and less observed especially when the Lévy index is less than 2, but is observed well when the index is equal to 2. Figure 13 reveals that the two energy barriers are roughly equivalent when $a < 2.0$. Figure 13(i) shows the variation in the effective energy barriers

versus the Lévy index a with the set of parameters AS_1 . The effective energy barriers increase slowly when the Lévy index a increases, and the behaviors strongly depend upon the Lévy index. For instance $\frac{\Delta U_1}{\Delta U_3}(a = 0.1) \equiv 1.2$, one concludes that the limit-cycle attractor with amplitude A_1 of the modified van der Pol oscillator is much more stable than the limit cycle attractor with amplitude A_3 (with respect to Lévy noise). The increase in the Lévy index will not modify the properties of the stability that we have just underlined, but the attractor around the limit cycle with amplitude A_1 becomes more and more stable when this index is close to 2. We will have gradually $\frac{\Delta U_1}{\Delta U_3}(a = 1.9) \equiv 2.34$, $\frac{\Delta U_1}{\Delta U_3}(a = 1.99) \equiv 7.3$ and $\frac{\Delta U_1}{\Delta U_3}(a = 2.0) \equiv 3.4$. Figure 13(ii) corresponds on the symmetric pseudo-potential and one shows the dependencies of the effective energy barriers versus the Lévy index a with the set of parameters S_1 . The behaviors of the effective energy barriers increase slowly with the increase of the Lévy index a , and depend upon the escape transitions. It appears that when the Lévy index a takes the value $a = 0.1$, the limit cycle amplitude A_1 is more stable than the limit cycle amplitude A_3 , (*i.e.* $\frac{\Delta U_1}{\Delta U_3} \equiv 1.22$), when the Lévy index increases moreover, the same scenario continues until the value $a < 1.0$, in which the opposite phenomenon occurs and the limit cycle amplitude A_3 becomes more stable, $\frac{\Delta U_1}{\Delta U_3} \equiv 0.9$. When the Lévy index more increases until $a = 1.75$, we have a situation reversal where the limit cycle amplitude A_1 becomes more stable since $\frac{\Delta U_1}{\Delta U_3}(a = 1.75) \equiv 1.52$. When $a \geq 1.8$, it is the limit cycle amplitude A_3 which returns stable that the limit cycle of amplitude A_1 . This cascade of scenarios appears in table V where we have grouped the behavior of the ratio of the energy barrier values for the two escapes transitions, in the case of asymmetric and symmetric pseudo-potentials. In order to make an equivalence between the depth of a pseudo-potential well and the stability of the attractor associated with this pseudo-potential sink, we will evaluate the time spend by a confined particle will put around each potential well, *i.e.* on each attractor.

Let us note that short and long might be very different. To measure the different properties, we compute the average persistence or residence time $R_{1,3}$ on the attractor with limit-cycle amplitude $A_{1,3}$ as

$$R_j = \frac{T_j}{T_1 + T_3}, \quad j = 1, 3 \quad (19)$$

where $T_{1,3}$ is the escape time from the first attractor A_1 (*i.e.* $T_1 = T_{esc}(A_1 \rightarrow A_3)$) or third attractor A_3 (*i.e.* $T_3 = T_{esc}(A_3 \rightarrow A_1)$). Figures 14 and 15 show the effects of the noise intensity on the dependencies the residence times $R_{1,3}$ as a function of the Lévy index, a for the asymmetric and the symmetric pseudo-potentials, respectively. For the case of asymmetric pseudo-potential (*i.e.* the parameters AS_1), for noise intensity around $D = 1/1000$ and with the Lévy index fix at

$a = 0.1$, we get $R_3(a = 0.1) = 0.659$, and obviously $R_1(a = 0.1) = 0.3402$, (see Fig. 14) *i.e.*, the system will spend 65.9% of the time on the third attractor A_3 and 34.02% on the first attractor A_1 . When we increase Lévy's index, the residence time on attractor A_1 increases while that on attractor A_3 decreases. It appears through Fig.14(i) that at $a = 0.6$, the system will spend the same time on the two attractors A_1 and A_3 , *i.e.* $R_1(a = 0.6) \equiv R_3(a = 0.6)$. By further increasing the Lévy index, R_1 continues to increase while R_3 continues to decrease, we will still have $R_1 > R_3$ when $a > 0.6$. By changing the intensity of the noise, *i.e.* $D = 1/100$, we will obtain the same scenario as the one described previously, but with the difference that the system will spend the same time on the two attractors, (*i.e.* $R_1 \equiv R_3$) when the Lévy index, a is around 0.7. Figure 15 shows the variation of the residence times $R_{1,3}$ as a function of the Lévy index for the symmetric pseudo-potential, with two values of the noise intensity: $D = 1/1000$ and $D = 1/100$. We note that unlike the case of asymmetric pseudo-potential, the system will take more time on the attractor A_3 because $R_3 > R_1$ when the index of Lévy increases. But we will note a small window of the Lévy index a where we observe $R_3 < R_1$, which can be neglected when the number of numerical iteration processes becomes very large.

IV. CONCLUSION

We have considered through numerical simulations the effects of Lévy noise on the birhythmic van der Pol system. After presenting the self-sustained model used, we briefly recalled the birhythmic properties on the free noise model. We then give the information about the Lévy noise process and indicates the algorithm we used to generate the Lévy noise. The Lévy probability density function was represented as a function of different Lévy stability parameters, showing its symmetric and asymmetric character. To find the effects of Lévy noise on the occurrence of large deviations, that is excursions from an attractor to another, we have modified the functional form of the *Arrhenius*-like behavior, Eqs.(13) and found that the escapes are governed, for the Lévy noise systems by the law Eq.(14), depends in addition to the noise intensity, D , to the Lévy parameters. Adding a random excitation, we have found that the system crosses the boundary between the basins of attraction (*i.e.*, moves across the unstable limit cycle with amplitude A_2). The mean time T_{esc} to escape from one limit-cycle attractor to the other has been estimated in the low-noise limit, and it is proposed as a measure of the attractors global stability. We have found that as in other systems that exhibit noise induced switches between two attractors, the escape times can be

very different and significantly depend to the Lévy index, α . It appeared that, increasing the Lévy index has the important influence on the birhythmic properties and then on the stability analysis. For instance, the pseudo-potential which initially was asymmetrical (symmetrical) becomes with the variation of the Lévy index, symmetric (asymmetrical). And therefore for the fixed value of the noise intensity, the means escape time has increased, decreased or remains almost constant depending on the shape of the resulting pseudo-potential well. By considering the variation in the mean escape time T_{esc} versus the inverse noise intensity $1/D$, the slope of the linear part has enabled us to summarize the results in the form of an effective activation energy barrier, which is function of the Lévy index α .

We conclude that.....

Conflict of Interest

The authors declare that they have no conflict of interest.

Acknowledgments

R.Y. undertook this work with the support of the German Academic Exchange Service(DAAD), Germany. He acknowledges the support of the Potsdam Institute for Climate Impact Research (PIK), Potsdam, Germany.

-
- [1] A. A. Dubkov, B. Spagnolo and V. Uchaikin, *Int. J. Bifurcation Chaos Appl. Sci. Eng.* **18**, 2649-2672 (2008).
- [2] A. La Cognata, D. Valenti, A. A. Dubkov and B. Spagnolo, "Dynamics of two competing species in the presence of Lévy noise sources", *Phys. Rev. E* **82**, 011121 (2010).
- [3] X. Yang and A. P. Petropulu, *IEEE Transactions on Signal Processing* **51**, 64 (2003).
- [4] V. Bhatia, B. Mulgrew, and A. Georgiadis, *Signal Processing* **86**, 835 (2006).
- [5] C. Li and G. Yu, in 2010 Second International Conference on Computer Modeling and Simulation , Vol. 4 (2010) pp. 386-390.
- [6] R. Saadane, M. E. Aroussi, and M. Wahbi, in 2015 3rd International Renewable and Sustainable Energy Conference (IRSEC) (2015) pp. 1-5
- [7] B. Chouri, M. Fabrice, A. Dandache, M. E. Aroussi, and R. Saadane, in 2014 International Conference on Multimedia Computing and Systems (ICMCS) (2014) pp. 1545-1550.
- [8] S. Luryi, O. Semyonov, A. Subashiev, and Z. Chen, *Phys. Rev. B* **86**, 201201 (2012).
- [9] A. V. Subashiev, O. Semyonov, Z. Chen, and S. Luryi, *Phys. Lett. A* **378**, 266 (2014).
- [10] D. S. Novikov, M. Drndic, L. S. Levitov, M. A. Kastner, M. V. Jarosz and M. G. Bawendi, *Phys. Rev. B* **72**, 075309 (2005).
- [11] X. Brokman, J.-P. Hermier, G. Messin, P. Desbiolles, J.-P. Bouchaud and M. Dahan, *Phys. Rev. Lett.* **90**, 120601 (2003).
- [12] M. Kuno, D. P. Fromm, H. F. Hamann, A. Gallagher and D. J. Nesbitt, *J. Chem. Phys.* **115**, 1028 (2001).
- [13] G. Messin, J. P. Hermier, E. Giacobino, P. Desbiolles and M. Dahan, *Opt. Lett.* **26**, 1891 (2001).
- [14] R. Metzler and J. Klafter, "The random walk's guide to anomalous diffusion a fractional dynamics approach", *Physics Reports* **339**, 1–77, (2000).
- [15] A. M. S. Mohammed, Y. R. Koh, B. Vermeersch, H. Lu, P. G. Burke, A. C. Gossard and A. Shakouri, *Nano Letters* **15**, 4269 (2015).
- [16] B. Vermeersch, A. M. S. Mohammed, G. Pernot, Y. R. Koh and A. Shakouri, *Phys. Rev. B* **91**, 085203 (2015).
- [17] Y. Elyassami, K. Benjelloun and M. El Aroussi, *Contemp. Eng. Sci.* **9**, 453 (2016).
- [18] A. Barone and G. Paternó, *Physics and Applications of the Josephson Effect* (Wiley, New York, 1982)

- [19] C. Guarcello, D. Valenti, A. Carollo and B. Spagnolo, J. Stat. Mech.: Theory Exp. 054012 (2016).
- [20] U. Briskot, I. A. Dmitriev, and A. D. Mirlin, Phys. Rev. B **89**, 075414 (2014).
- [21] R. Yamapi and G. Filatrella, Noise effects on a birhythmic Josephson junction coupled to a resonator, Phys. Rev. E **89**, 052905 (2014).
- [22] R. L. Kautz, Thermally induced escape: The principle of minimum available noise energy. Phys. Rev. A **38**, 2066 (1988).
- [23] R. L. Kautz Quasipotential and the stability of phase lock in nonhysteretic Josephson junctions. J. Appl. Phys. **76**, 5538 (1994); doi: 10.1063/1.357156
- [24] Yamapi R, Filatrella G, Aziz-Alaoui MA, Cerdeira HA. Effective Fokker-Planck equation for birhythmic modified van der Pol oscillator. Chaos 2012; 22: 043114.
- [25] R. Yamapi, G. Filatrella, and M. A. Aziz-Aloui, Global stability analysis of birhythmicity in a self-sustained oscillator, CHAOS **20**, 013114 (2010).
- [26] Mbakob Yonkeu R, Yamapi R, Filatrella G, Tchawoua C. Stochastic Bifurcations induced by correlated Noise in a Birhythmic van der Pol System. Commun. Nonlinear Sci Numer. Simulat. 2016; 33: 70–84.
- [27] R. Mbakob Yonkeu, R. Yamapi, G. Filatrella and C. Tchawoua, Effects of a Periodic Drive and Correlated Noise on Birhythmic van der Pol Systems, submitted on Physica A **466** (2017) 552-569.
- [28] A. V. Chechkin, V. Y. Gonchar, and M. Szydlowsky, Phys. Plasmas **9**, 78 (2002);
- [29] A. V. Chechkin and V. Yu. Gonchar, Zh. Eksp. Teor. Fiz. **118**, 3 (2000).
- [30] Yiqun Sun and Xiang Zhou, An Improved Adaptive Minimum Action Method for the Calculation of Transition Path in Non-gradient Systems, arXiv:1701.04044v6
- [31] X. Wan, B. Zheng and G. Lin, Commun. Comput. Phys. **23** 408–439 (2018).
- [32] M Högele, I. Pavlyukevich, The Exit Problem from a Neighborhood of the Global Attractor for Dynamical Systems Perturbed by Heavy-Tailed Lvy Processes, Journal Stochastic Analysis and Applications **32** 163–190 (2014) doi: 10.1080/07362994.2014.858554 ; M. Högele and Ilya Pavlyukevich, arXiv:1405.5433v1 ; M. Högele and I. Pavlyukevich, Metastability in a class of hyperbolic dynamical systems perturbed by heavy-tailed Lévy type noise, Stochastics and Dynamics **15**, 1550019 (2015). doi 10.1142/S0219493715500197
- [33] F. Morán and A. Goldbeter, Onset of birhythmicity in a regulated biochemical system, Biophysical Chemistry, **20**, 149-156 (1984).
- [34] F. Kaiser and C. Eichwald, Int. J. Bifurc. Chaos **1**, 485 (1991).

- [35] C. Eichwald and F. Kaiser, *Int. J. Bifurc. Chaos* **1**, 711 (1991).
- [36] H. G. Enjieu Kadji, R. Yamapi and J. B. Chabi Orou, *Chaos* **17**, 033113 (2007).
- [37] H. G. Enjieu Kadji, J. B. Chabi Orou, R. Yamapi and P. Woafu, *Chaos, Solitons and Fractals* **32**, 862 (2007).
- [38] R. Yamapi, B. R. Nana Nbandjo and H. G. Enjieu Kadji, *Int. J. Bifurc. Chaos*, **17(4)** 1343 (2007).
- [39] H. G. Enjieu Kadji, Synchronization dynamics of nonlinear self-sustained oscillations with applications in physics, engineering and biology, PhD Dissertation of Physics, Institut de Mathématiques et de Sciences Physiques (I.M.S.P.), Porto-Novo, Université d'Abomey-Calavi, June 2006, Benin.
- [40] F. Kaiser, Coherent oscillations in biological systems: Interaction with extremely low frequency fields, *Radio Sci.* **17**, 17S (1981).
- [41] V.-X. Li, A. Goldbeter, Oscillatory isozymes as the simplest model for coupled biochemical oscillators, *J. Theor. Biol.* **138**, 149 (1989).
- [42] F. Kaiser, Coherent Excitations in Biological Systems: Specific Effects in Externally Driven Self-Sustained Oscillating Biophysical Systems (Springer- Verlag, Berlin, Heidelberg, 1983).
- [43] F. Kaiser, Theory of resonant effects of RF and MW energy, in *Biological Effects of an Dosimetry of Nonionizing Radiation*, eds. Grandolfo, M., Michaelson, S. M. and Rindi, A. (Plenum Press, NY, 1983), p. 251.
- [44] F. Kaiser, The role of chaos in biological systems, in *Energy Transfer Dynamics*, eds. Barret, T. W. and Pohl, H. A. (Springer, Berlin, 1987), p. 224.
- [45] F. Kaiser, Nichtlineare resonanz und chaos. Ihre relevanz für biologische funktion, *Kleinheubacher Berichte* **32**, 395 (1989).
- [46] D. Applebaum, *Lévy Processes and Stochastic Calculus*, 2nd ed.(New York Cambridge University Press, 2009).
- [47] R. Weron, Lévy-stable distributions revisited: tail index > 2 does not exclude the Lévy-stable regime, *International Journal of Modern Physics C* **12**, 209–223, (2001).
- [48] A. Janicki, A.Weron, *Simulation and chaotic behavior of α -stable stochastic processes*, Marcel Dekker, New York, 1994.
A. Janicki, *Numerical and Statistical Approximation of Stochastic Differential Equations with Non-Gaussian Measures*, HSC Monograph, Wroc law, 1996
- [49] Y. Xu, Y. Li, J. Li, J. Feng, H. Zha, The Phase Transition in a Bistable Duffing System Driven by Lévy Noise, *J Stat Phys* **158**, 120-131, (2015).

- [50] K. Jacobs, Stochastic processes for physicists: Understanding Noisy Systems, Cambridge University Press, New York, ISBN-13 978-0-521-76542-8, (2010)
- [51] H. Fröhlich, Coherence and the action of enzymes. In: G.R. Welch, Editor, The Fluctuating Enzyme, Wiley, New York, p. 421 (1986).
- [52] F. Kaiser, Z Naturforsch A **33**, 294 (1978).
- [53] R. Graham and T. Tél, Weak-noise limit of Fokker–Planck models and nondifferentiable potentials for dissipative dynamical systems. Phys. Rev. A **31**, 1109 (1985).
- [54] Yamapi R, Chéagé Chamgoué A, Filatrella G and Wofo P. Coherence and stochastic resonance in a birhythmic van der Pol system. Eur.Phys. J. B. **90**, 153 (2017).
- [55] R. Mbakob Yonkeu, R. Yamapi, G. Filatrella and C. Tchawoua, Pseudopotential of birhythmic van der Pol type systems with correlated noise. Nonlinear Dynamics, 2016; 84(2): 627–639.
- [56] C. Guarcello, D. Valenti, B. Spagnolo, V. Pierro, and G. Filatrella “Josephson-based threshold detector for Lévy distributed fluctuations”, arXiv:1802.01095v1 [cond-mat.mes-hall]
- [57] Aleksei V. Chechkin, V. Yu. Gonchar, J. Klafter and R. Metzler. Barrier crossing of a Lévy flight. Europhys. Lett., 72(3), pp. 348-354 (2005). DOI:10.1209/epl/i2005-10265-1
- [58] Aleksei V. Chechkin, Oleksii Yu. Sliusarenko, Ralf Metzler and Joseph Klafter, Barrier crossing driven by Lévy noise: Universality and the role of noise intensity. Phys. Rev. E 75, 041101 (2007)

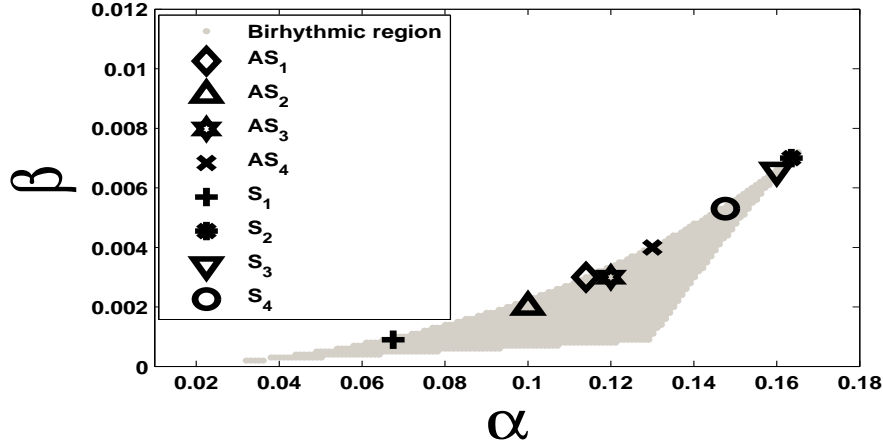


Figure 1: *Parameter region of the single limit cycle (white area) and three limit cycles (gray area) with $\mu = 0.01$ as obtained from simulations of Eq.(3). The symbols refer to the parameter sets investigated in this work, see Tables I and II. The other parameter is $\mu = 0.01$.*

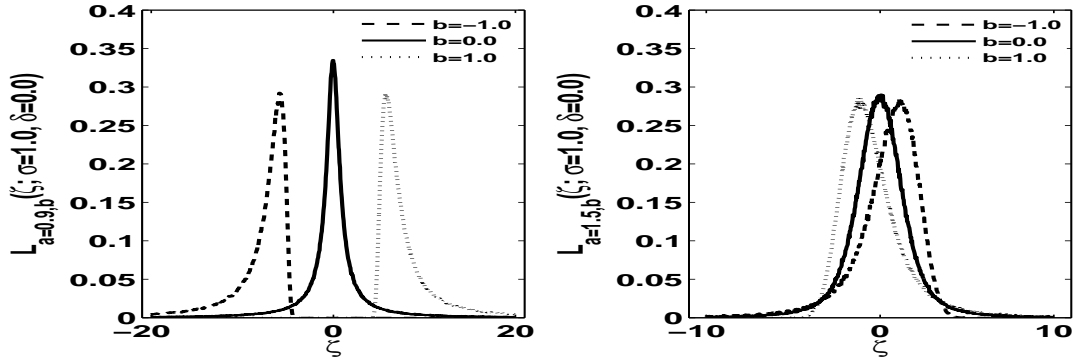


Figure 2: *Sample a -stable probability density functions (PDF) with $a = 0.9$ (left panel) and $a = 1.5$ (right panel). For $b = 0$ distributions are symmetric, while for $b \neq 0$ they are asymmetric functions.*

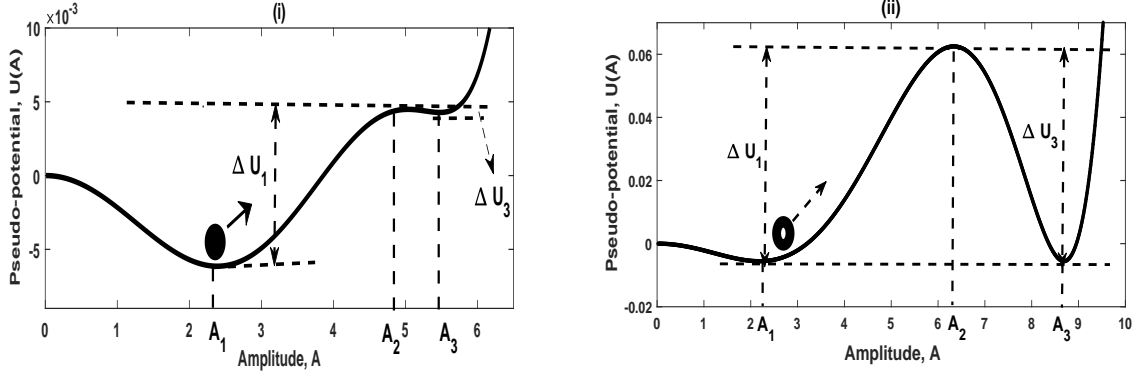


Figure 3: The effective pseudo-potential $U(A)$ versus the amplitude A for the free-noise self-sustained oscillator with multi-limit-cycles, while (i) correspond to the asymmetric potential with the AS_1 parameters and (ii) to the symmetric potential with the SS_1 parameters. The other parameter is $\mu = 0.01$.

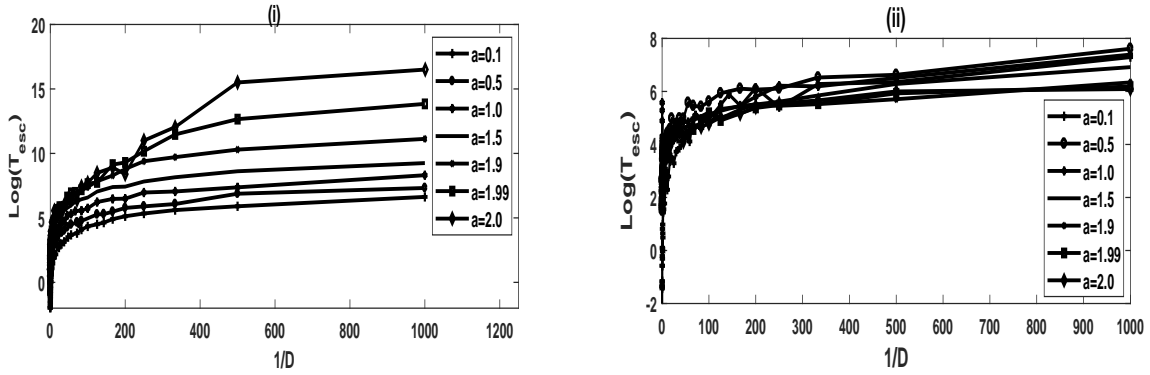


Figure 4: Mean escape time versus the noise intensity $1/D$ for the asymmetric quasi-potential with several different values of the Lévy index, a , (i) correspond of the escape transition $A_1 \rightarrow A_3$ and (ii) for the escape transition $A_3 \rightarrow A_1$. The other parameter is $\mu = 0.01$.

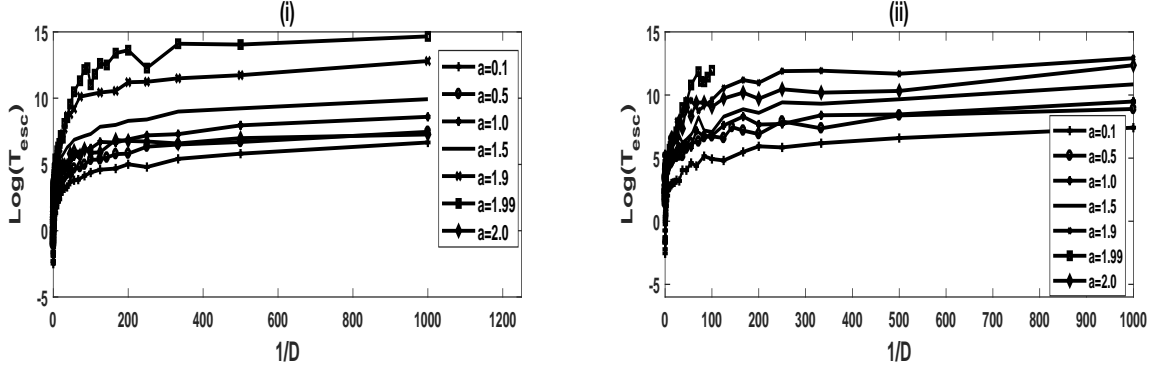


Figure 5: Mean escape time versus the noise intensity $1/D$ for the symmetric quasi-potential with several different values of the Lévy index, α , (i) correspond of the escape transition $A_1 \rightarrow A_3$ and (ii) for the escape transition $A_3 \rightarrow A_1$. The other parameter is $\mu = 0.01$.

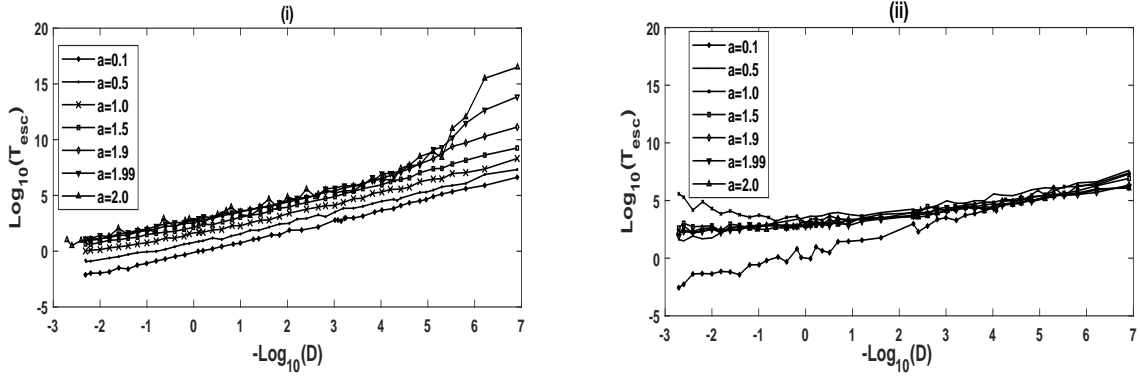


Figure 6: Mean escape time versus the noise intensity D for the asymmetric quasi-potential with several different values of the Lévy index, α , (i) correspond of the escape transition $A_1 \rightarrow A_3$ and (ii) for the escape transition $A_3 \rightarrow A_1$. The other parameter is $\mu = 0.01$.

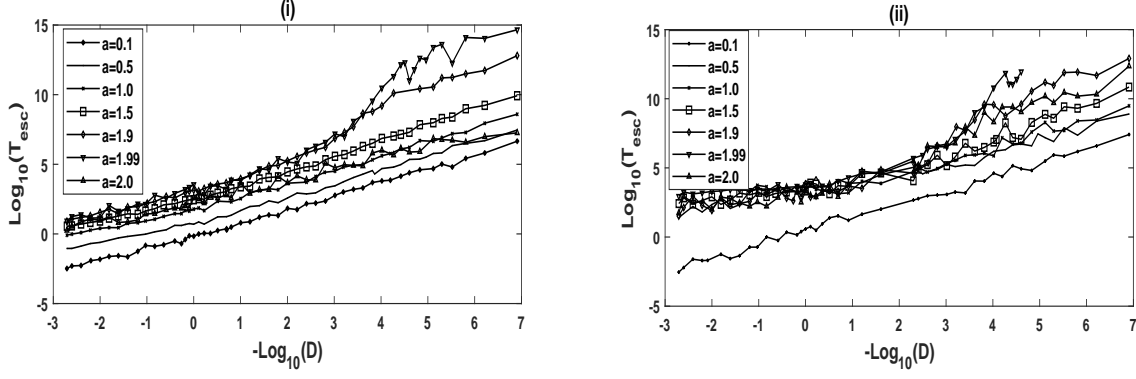


Figure 7: Mean escape time versus the noise intensity D for the symmetric quasi-potential with several different values of the Lévy index, a , (i) correspond of the escape transition $A_1 \rightarrow A_3$ and (ii) for the escape transition $A_3 \rightarrow A_1$. The other parameter is $\mu = 0.01$.

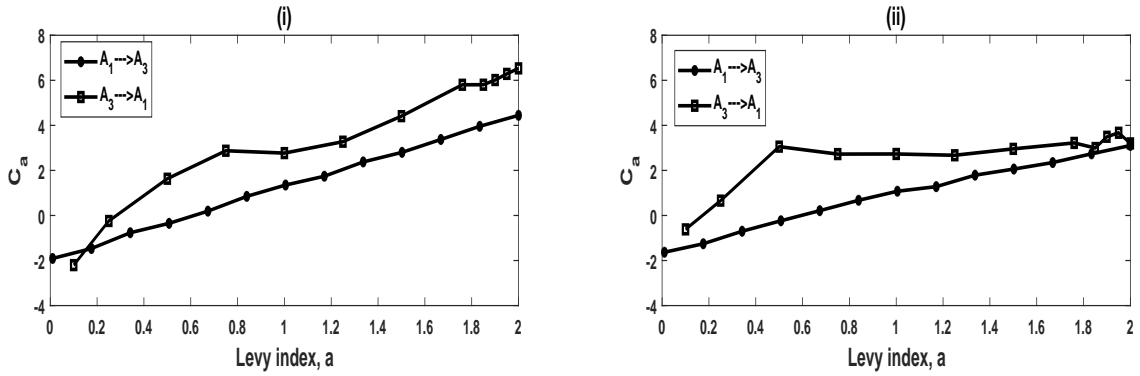


Figure 8: Dependence of the scaling exponent C_a versus the Lévy index, a . (i) correspond of the asymmetric pseudo-potential and (ii) for the symmetric pseudo-potential. The other parameter is $\mu = 0.01$.

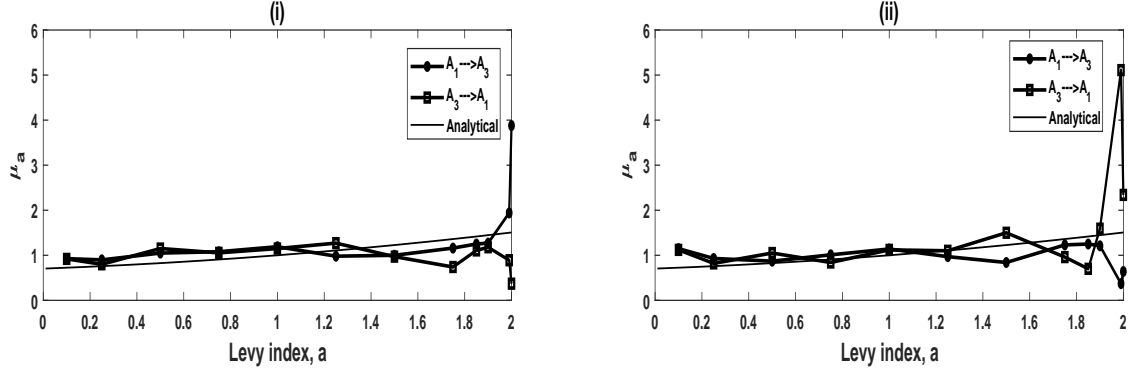


Figure 9: Dependence of the scaling exponent μ_a versus the Lévy index, a . (i) correspond of the asymmetric pseudo-potential and (ii) for the symmetric pseudo-potential. The analytic prediction of the solid line refers to Eq.(14).

GF: check the above statement is correct.

The other parameter is $\mu = 0.01$.

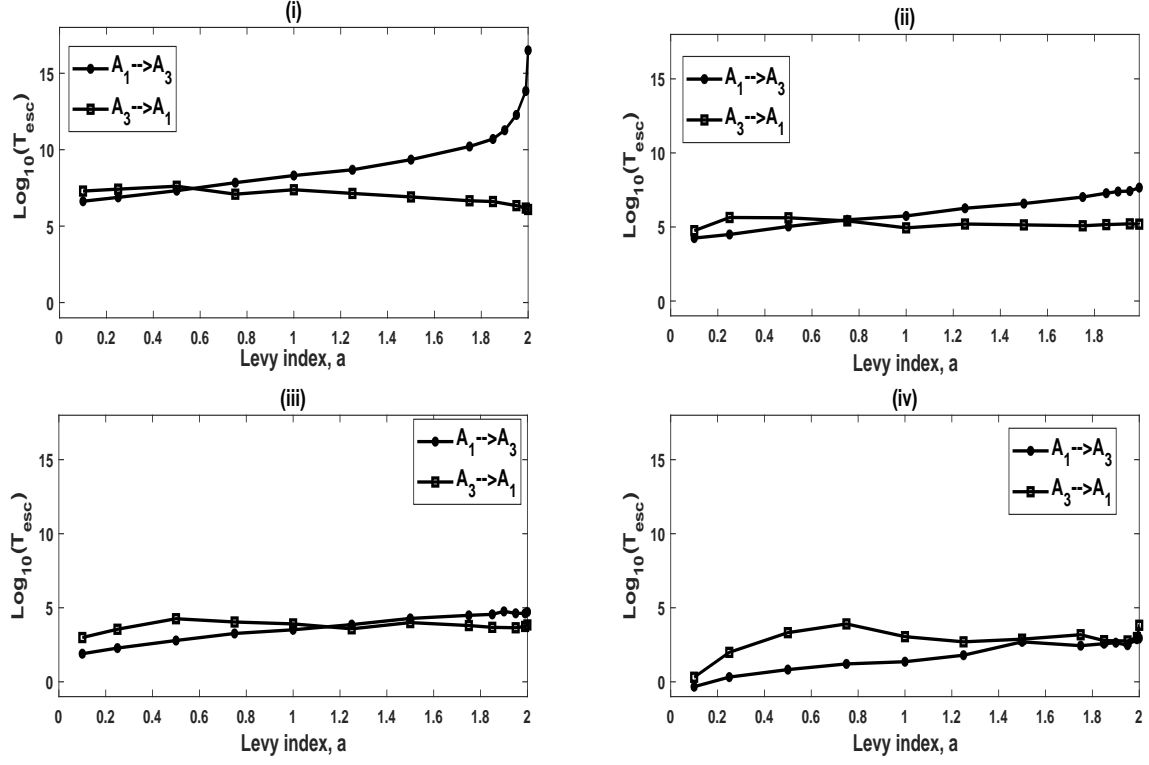


Figure 10: Effects of the Lévy noise intensity on the variation of the mean escape time versus the Lévy index a for the asymmetric quasi-potential (i): $D = 0.001$; (ii): $D = 0.01$; (iii): $D = 0.1$; (iv): $D = 1.0$. The other parameter is $\mu = 0.01$.

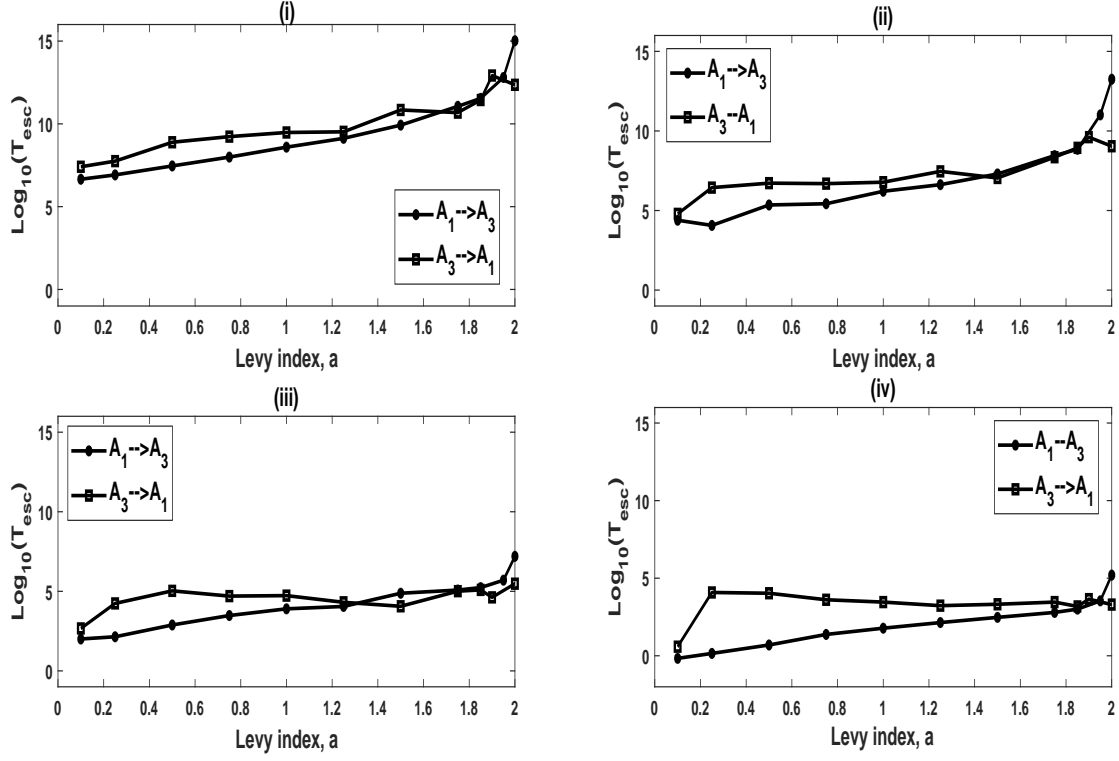


Figure 11: Effects of the Lévy noise intensity on the variation of the mean escape time versus the Lévy index a for the symmetric quasi-potential (i): $D = 0.001$; (ii): $D = 0.01$; (iii): $D = 0.1$; (iv): $D = 1.0$. The other parameter is $\mu = 0.01$.

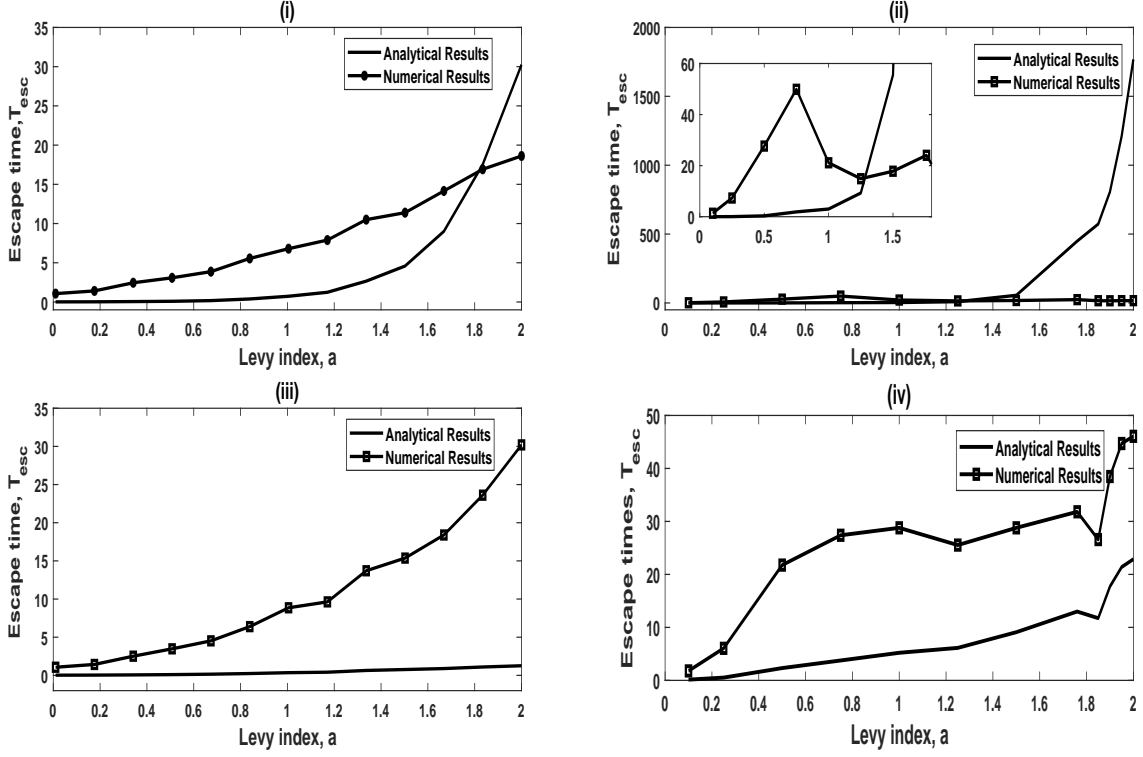


Figure 12: Comparison between analytical and numerical results for the asymmetric quasi-potential (i); (ii), and the symmetric potential (iii), (iv). (i, ii) $A_1 \rightarrow A_3$; (ii, iv) $A_3 \rightarrow A_1$ with $D = 1.0$.

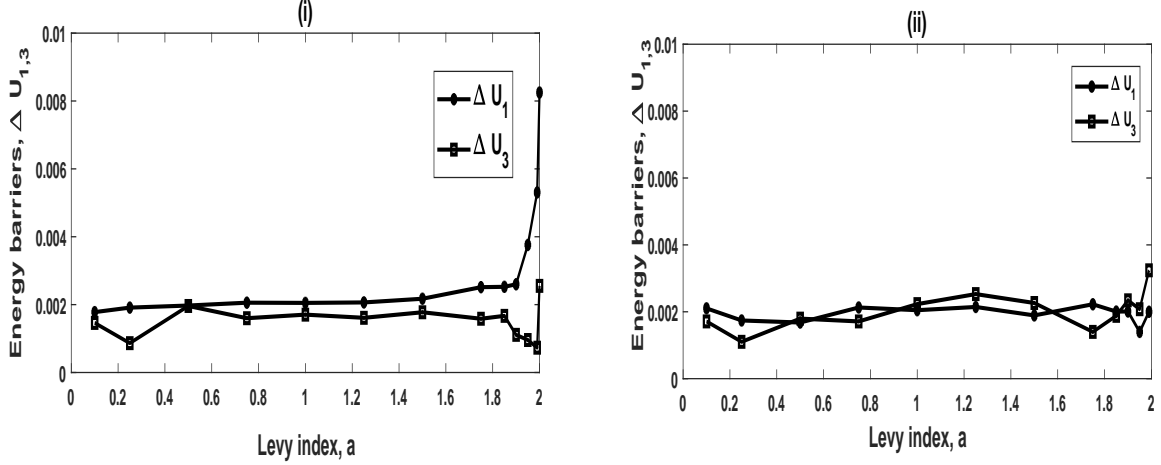


Figure 13: Variation of the energy barriers versus the Lévy index, a . Note that (i) correspond for the asymmetric quasi-potential, while (ii) is for the symmetric potential. The other parameter is $\mu = 0.01$.

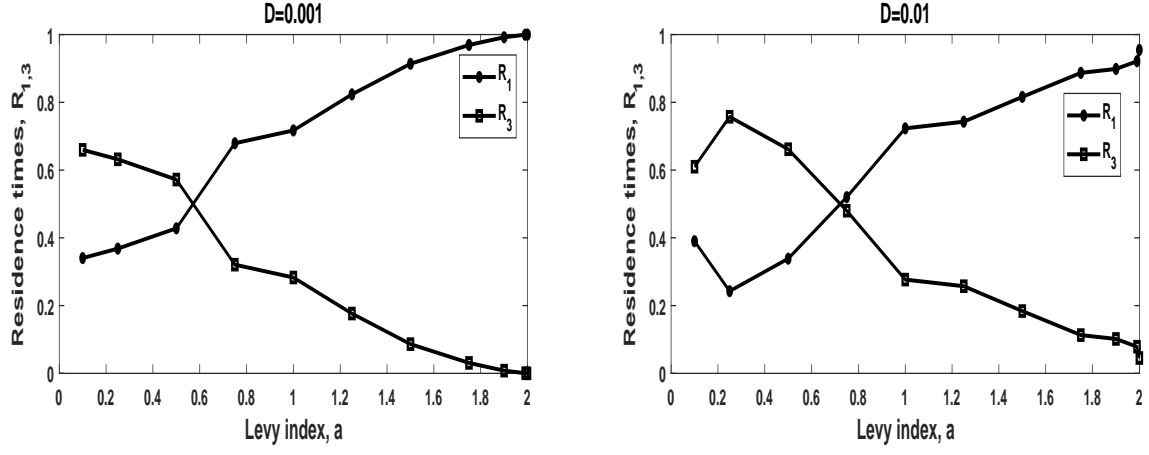


Figure 14: Residence times $R_{1,3}$ as a function of the Lévy index, a for different values of the noise intensity, D , for the asymmetric quasi-potential. The other parameter is $\mu = 0.01$.

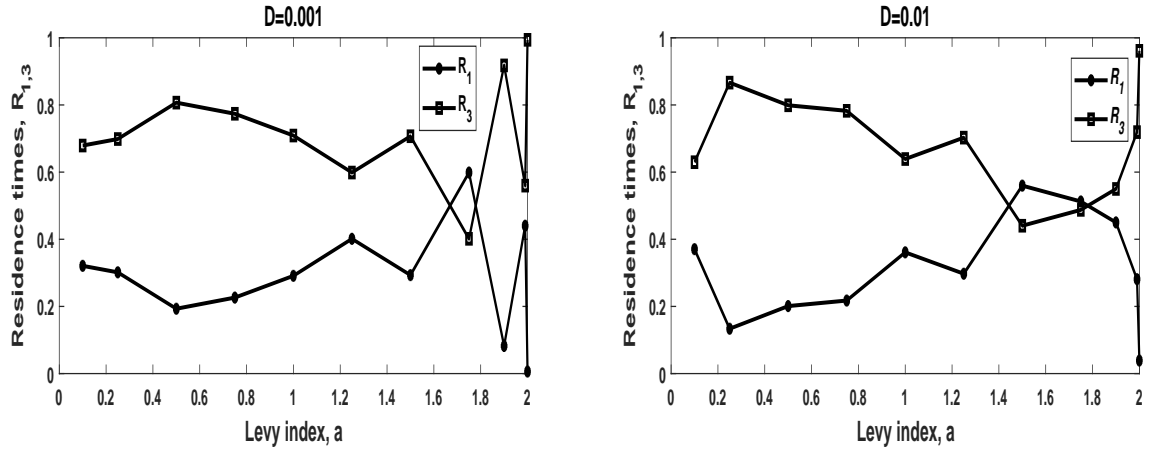


Figure 15: Residence times $R_{1,3}$ as a function of the Lévy index, a for different values of the noise intensity, D , for the symmetric quasi-potential. The other parameter is $\mu = 0.01$.